Journal of Alloys and Compounds 506 (2010) 653–660

Contents lists available at ScienceDirect

Journal of Alloys and Compounds

journal homepage: www.elsevier.com/locate/jallcom

Synthesis of AlN–TiN nanostructured composite powder by reactive ball milling and subsequent thermal treatment

H. Amini Mashhadi[a,*], P. Manikandan[a], R. Suetsugu[a], S. Tanaka[b], K. Hokamoto[c]

[a] Graduate School of Science and Technology, Kumamoto University, 2-39-1 Kurokami, Kumamoto, Japan
[b] Faculty of Engineering, Kumamoto University, 2-39-1 Kurokami, Kumamoto, Japan
[c] Shock Wave and Condensed Matter Research Center, Kumamoto University, 2-39-1 Kurokami, Kumamoto, Japan

ARTICLE INFO

Article history:
Received 18 January 2010
Received in revised form 7 July 2010
Accepted 7 July 2010
Available online 15 July 2010

Keywords:
Nanostructured composite
Mechanical alloying
Mechanochemical processing
Solid-state reaction

ABSTRACT

In the present article, synthesis of AlN–TiN nanostructured composite by high-energy ball milling process (HEM) of Ti and AlN by 1:1 molar ratio and subsequent heat treatment was investigated. The microstructural evolution of samples was studied by scan electron microscopy (SEM) and energy dispersive X-ray analysis (EDS), composition map analysis by electron probe micro-analyzer (EPMA) and phase determination using X-ray diffraction (XRD) patterns. It was found that a Ti(Al,N) solid solution was formed at the early stages of milling and while Al causes the Ti lattice to contract, N has the opposite effect. The nonlinear variation of interplanar distance and *c*/*a* ratio of Ti is considered due to the competition between these two processes during MA and finally led to complete dissolution of Al and only 1 at.% of N in Ti lattice.

On further milling, mechanochemical reaction between Ti solid solution and AlN took place in the gradual mode which led to the formation of TiN with an average crystallite size of 10 nm. It is generally acknowledged that the reactions between Ti and AlN includes three stages: (i) reduction of AlN under the effect of Ti; (ii) diffusion of dissolved Al and N atoms into the Ti lattice and (iii) reaction between Al,Ti and N. XRD results revealed that annealing of the milled powders resulted in greater formation of "in situ" TiN particles from supersaturated solid solution and increases the crystallite size of TiN from 10 nm to 14.62 nm.

1. Introduction

There has been increasing interest in refractory materials such as carbides, nitrides, and borides owing to their exceptional hardness and stability at high temperatures. Especially, nitride ceramics such as TiN and AlN have been developed due to their specific properties and potential application [1]. However, single-phase refractory materials have reached their optimum stage and attention has now turned to composite refractory materials. Particulate reinforced CMCs containing hard ceramic or ductile metal/intermetallic inclusions exhibit several advantages compared to single-phase ceramics, e.g. high fracture toughness and strength, enhanced thermal shock resistance and high wear resistance [2,3].

In addition, nanocrystalline refractory materials have recently received much attention due to their improved mechanical properties, and there is a growing interest in the investigation of nanocomposites due to the superior mechanical properties [4,5]. A variety of techniques for preparing nanocrystalline materials have been proposed over the past decade.

Mechanical alloying (MA) is a versatile processing technique for the fabrication of novel materials such as nanocomposites, and high-energy ball milling has been recognized as an effective way of producing nanocrystalline, amorphous and other non-equilibrium structured powders mainly through a solid-state reaction [6,7]. Particularly, high-energy ball milling accompanying chemical reactions, i.e. mechanochemical processing, is considered to be very effective for preparing nanostructured composite powders containing more than two phases [8]. In this process, elemental blends are milled by high-energy collisions among balls to stimulate different types of reaction by diffusion at atomic and nanocrystalline levels [9,10]. This technique can be used to induce displacement reactions at much lower temperatures than normally required. This allows the in situ formation of composites during milling or during subsequent thermal processing of milled powders [11,12]. A variety of nanostructured composites have been synthesized by mechanochemical processing of the respective powders for a few hours at room temperature [13–17].

* Corresponding author. Tel.: +81 80 4276 1706; fax: +81 96 342 3293.
E-mail addresses: hossein1@shock.smrc.kumamoto-u.ac.jp, amir_hie@yahoo.com (H.A. Mashhadi).

0925-8388/$ – see front matter © 2010 Elsevier B.V. All rights reserved.
doi:10.1016/j.jallcom.2010.07.037

Titanium nitride (TiN) has many desirable properties, such as good corrosion resistance, heat resistance, low chemical reactivity, wear resistance property [12,18,19], high hardness (≈20 GPa) with a low friction coefficient[20,21], good conductivity with high melting temperature (2927 °C) and barrier properties [22]. On the other hand AlN possesses excellent thermal conductivity, low thermal expansion, high hardness, good electrical resistance, high melting point and good oxidation resistance at elevated temperatures [23–26].

In recent years, AlN–TiN composites have been exciting more interests in the field of wear-resistant components because the mechanical properties, such as hardness, fracture toughness and friction coefficients which are superior to those of either AlN or TiN single-phase ceramic [27–29]. There are several research works on the interfacial reaction between Ti and AlN but much of them concentrate on studies in the formation of coating [30–35]. Direct mixing of Ti and AlN powders leads to in situ formation of TiN; hence, the MA process provides nanosized powders with rough and reactive surfaces as well as uniform distribution of different phases.

In the present study, the production of AlN–TiN nanostructured composite by mechanochemical reaction between Ti and AlN powders by high-energy ball milling and subsequent annealing was investigated. It is expected that dissociated nitrogen in AlN reacted with elemental Ti powder to form in situ TiN as a consequence of the very strong affinity between Ti and N, and that prolonging milling time allowed nanocrystalline structure formation.

2. Experimental procedure

The raw materials used in this study were 99.7% pure Ti powder (Sumitomo Titanium Corporation, Japan) with a particle size of less than 45 μm, and agglomerated AlN powder (Wako Chemicals, USA). The mixture of Ti and AlN powders were prepared in a glove box under a purified argon atmosphere for the stoichiometric reaction to take place: Ti + AlN → Al + TiN, with a molar ratio of 1:1 mixture and 1% stearic acid (Wako Pure Chemical Industries Ltd., Japan) as process control agent (PCA). The initial mixed powders were then charged and sealed in a stainless steel vial (500 ml) together with 25 stainless steel balls (10 mm). The ball to powder weight ratio was maintained as 10:1. The ball milling experiments were performed in a high-energy planetary ball mill (Fritsch 6) at rotation speed of 250 rpm. Separate samples were milled for 9 ks, 18 ks, 36 ks, 72 ks, 144 ks and 360 ks. After the allotted time, the powders were removed from the mills, and a small amount of powder was taken for characterization. Phase transformation and crystallite size evaluation during milling were determined by X-ray diffraction (XRD) with Cu Kα radiation (λ = 1.5405 Å). The crystallite size of powder during milling was determined from broadening of XRD peaks by Scherrer equation [36]:

$$B\cos\theta = \frac{0.9\lambda}{D} \quad (1)$$

where B is the full-width at half maximum intensity, λ the wavelength of the X-ray used, D the average crystallite size and θ the Bragg angle. The morphology of the mechanically alloyed powder samples was examined by scanning electron microscopy (SEM) in a JEOL (JCM-5700) at an accelerating voltage of 15 kV with an energy dispersive X-ray spectrometer (EDS) as well as EPMA measurements on a JEOL JXA 8900R microprobe with a wavelength dispersive spectrometer for material characterization.

3. Results and discussion

3.1. X-ray diffraction analysis and reaction mechanism

AlN–TiN nanostructured composite was synthesized by mechanochemical reaction during ball milling of a stoichiometric mixture of Ti and AlN according to the following reactions:

$$\mathrm{Ti} + \mathrm{AlN} = \mathrm{Al} + \mathrm{TiN}, \quad \Delta G^{\circ}_{298} = -22.158\ \mathrm{kJ\,mol^{-1}} \quad (2)$$

According to thermodynamics, if a reaction occurs spontaneously, the change in the Gibbs free energy of formation (ΔG) between reactants and products must be less than zero. Based on the thermodynamic data the above reaction may occur even at room temperature [37]. The occurrence of the reaction at ambient temperature is limited by kinetic considerations. MA can provide the means to substantially increase the reaction kinetics of the reduction reaction [7].

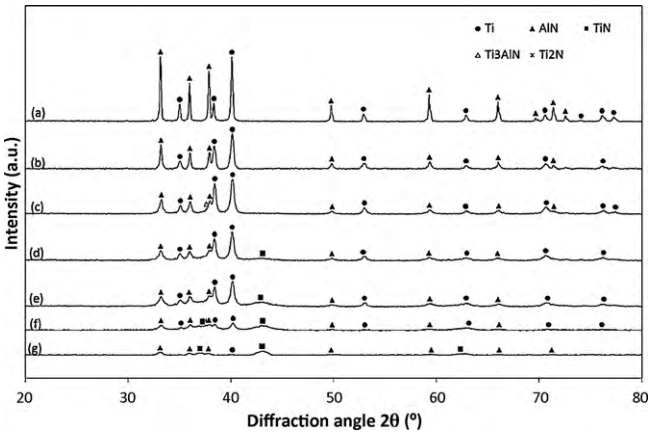

Fig. 1. XRD patterns of Ti + AlN mixture milled for different times: (a) mixed powder; (b) 9 ks; (c) 18 ks; (d) 36 ks; (e) 72 ks; (f) 144 ks; (g) 360 ks.

Fig. 1 shows the XRD patterns of powder mixture after different MA times. Fig. 1a relates to the mixture of starting materials (Ti and AlN). Obviously the starting materials contain coarse polycrystalline grains of Ti and AlN, suggested by the sharp diffraction peaks of powder mixture. There is no evidence of reaction between Ti and AlN until 18 ks, at which a small amount of Ti_3AlN phase could be detected, as shown in Fig. 1c; this, however, disappeared at the next stage of MA. With increasing milling time, the intensity of Ti and AlN peaks decreased and their width increased due to a decrease in crystallite size and enhancement of lattice strain. After 36 ks of milling, a trace of TiN peak at $2\theta = 42.79^{\circ}$ appeared besides main peak of titanium which was formed "in situ", directly during the MA process. The formation of TiN at ambient temperature signifies that the mixing of reactants takes place on a nanometer scale and considerably reduces the diffusion path length. On continued milling until 144 ks, the powder seemed to start losing crystalline (Fig. 1e). Further milling up to 360 ks (Fig. 1g) led to amorphous like solid solution phases. It has been reported that the presence of nitrogen atoms speeds up the amorphization [38]. It is worth noting that the amorphous phase is obtained when the N content in the compound is too high to be accommodated within the α-Ti lattice but too low to allow the formation of the cubic structure, i.e. understoichiometric relative to the Ti–Al–N compound [39]. Therefore this study did not complete generation of a full amorphous structure due to the formation of titanium nitride as a stoichiometric phase. It can also be seen that after 360 ks of milling time, the peaks of Ti have almost disappeared, implying that a reaction between Ti and AlN has taken place. Furthermore, it is observed that the peak of TiN increased in intensity, also confirming that Ti has reacted with AlN.

However the XRD patterns show a significant portion of AlN particles remained even after prolonged milling. This could be attributed to the partial reaction between Ti and AlN because of the low adiabatic temperature and insufficient milling intensity to activate the exchange reaction. As mentioned above, the displacement reaction during milling could be represented as reaction (2). Munir [40] proposed a simple guideline to determine whether or not a self-propagating reaction might occur for a certain system. According to his proposal, the reaction can start without additional energy from an exterior source when $-\Delta H/\mathrm{Cp}$ is above 2000 K. The $-\Delta H/\mathrm{Cp}$ value of reaction (2) was calculated as about 300 K, indicating that it could not progress via mechanically induced self-propagating reaction (MSR) and it underwent the gradual mode. In other words, the accumulated energy of powders mechanically alloyed for even up to 360 ks is insufficient to complete the transformation. Hence, a considerable amount of milling energy

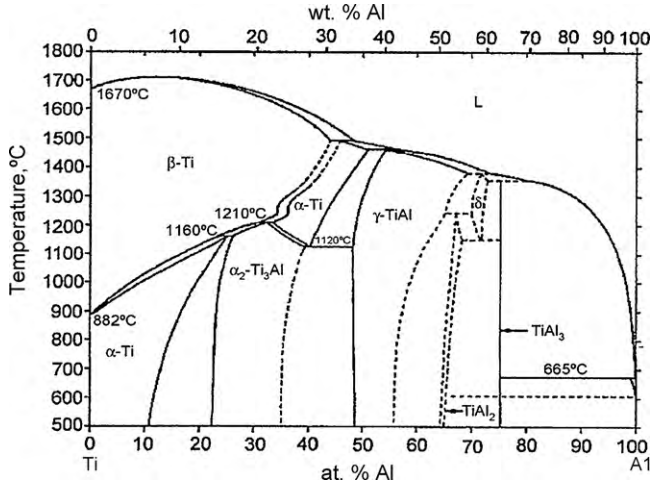

Fig. 2. Ti–Al phase diagram [43].

is consumed by fracturing the AlN and Ti particles; leaving the increased kinetic energy provided during MA in sufficient for completion of the reaction.

Furthermore, it is reasonable to assume that once there is no other nitrogen provider except AlN during MA, Ti merely seizes nitrogen atoms from AlN particles to form TiNx (x = 0.42–1) [41]. Beside this, both the covalent nature of AlN and the strong affinity of Al to N cause low diffusion rates. Such a conclusion is in agreement with the thermal data [42] and Ti–N binary phase diagram [41]. There is also no evidence of the formation of Al in diffraction spectra even after 360 ks MA (Fig. 1g). This result is in agreement with another work of the authors in which higher MA parameters (BPR 30:1 and RPM 600) were used to increase the frequency of the elementary processing events (collisions). This is related to the solubility of Al atoms in Ti lattice during MA. From the Ti–Al phase diagram shown in Fig. 2, it can be seen that Al has an extended solubility in Ti, while Ti has a limited solubility in Al. Displacement of the strongest reflection peak of Ti(1 0 1) towards higher angles (2θ = 40.10° to 2θ = 40.14°) after 360 ks MA time shows that the lattice parameter of Ti(Al,N) solid solution decreased with increasing milling time. According to Pearson and Raynor [44], the lattice parameter of Ti–Al solid solution decrease with increasing aluminum content. This behavior is a consequence of the substitution of Ti atoms by the smaller size Al atoms within the α-Ti lattice [45], leading to the contraction of Ti lattice and this is indicated by the shift of titanium peak to higher angle. By using XRD pattern, the *hcp* lattice parameters of Ti are found to be a = 0.2946 nm and c = 0.4676 nm after 144 ks MA time. These values are lower than α-Ti parameters (a = 0.2950, c = 0.4686 nm), which indicates the formation of Ti(Al) solid solution.

The calculated lattice parameters of the Ti(1 0 1) compared with that obtained from the initial powder of titanium, are reported in Table 1. The titanium cells parameters differ considerably between the milled powders and mixed powder (initial powder), namely the (a) and in particular the (c) parameters, and thus the (c/a) ratio of the 144 ks MA powder is significantly lower than the standard values (in our case, the mixed powder).

Fig. 3 shows the variation of the parameters (a) and (c) with the Ti(Al) solid solution [44]. It is found that aluminum from the decomposed AlN particles was completely dissolved in the hcp-Ti lattice, according to the maximum solubility of aluminum in titanium by MA which has been reported in the literature [7]. In contrast, it is found that the position of titanium Bragg peaks shifts to lower angles after 18 ks and 144 ks of milling time. Displacement of Ti(1 0 1) peak toward lower angles is shown in Fig. 4. This

Table 1
Calculated cell parameters of Ti(1 0 1) for different MA time together with literature standard.

Sample condition (ks of MA time)	Cell parameters of α-Ti		
	a (Å)	c (Å)	c/a
9	2.9489	4.6947	1.5919
18	2.9472	4.6781	1.5873
36	2.9457	4.6988	1.5951
72	2.9512	4.6795	1.5856
144	2.9462	4.6760	1.5766
Ti mixed powder	2.9554	4.6940	1.5883
α-Ti[a]	2.950	4.6866	1.588

[a] From JCPDS standard.

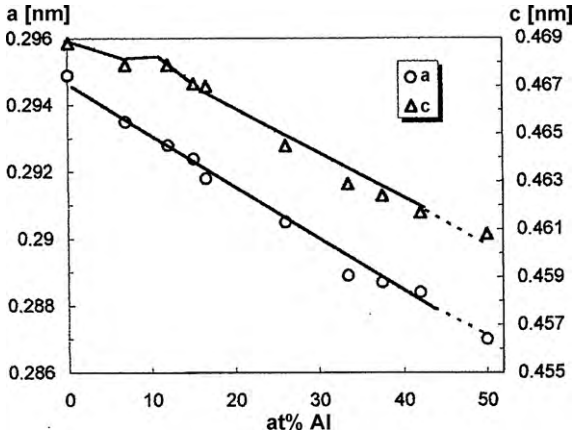

Fig. 3. Dependence of a and c parameters of Ti(Al) solid solution vs. aluminum content [44].

is related to the opposite effect of nitrogen atoms on titanium lattice, due to the interstitial dissolution of N atoms into Ti lattice which resulted in Ti(N) solid solution and increase the lattice parameter of titanium. This is in contract with the other research works [46,47]. According to the binary phase diagram representing thermodynamic equilibrium, at equilibrium state, the α-Ti lattice is only able to dissolve about 3–4 at.% of nitrogen at high temperature (above 800 K) [48]. However, as mechanical alloying is a thermodynamically non-equilibrium process, a metastable oversaturated solid solution of nitrogen and aluminum in titanium can be obtained at high concentrations well above those predicted by thermodynamics. In the case of nitrogen, the accommodation of the nitrogen atoms in interstitial octahedral α-Ti sites causes lattice expansion which explicates the shift of the diffraction peaks

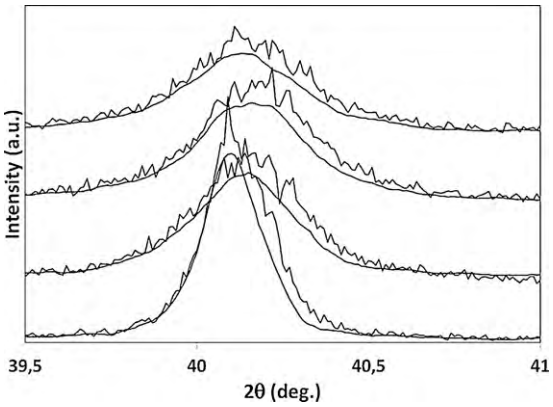

Fig. 4. Displacement of Ti(1 0 1) peak to lower angles.

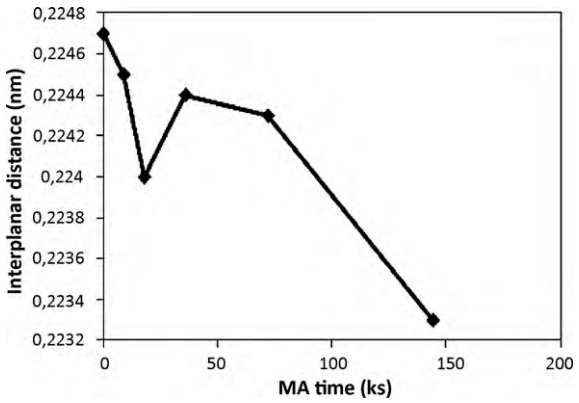

Fig. 5. Interplanar distance of Ti(1 0 1) vs. MA time.

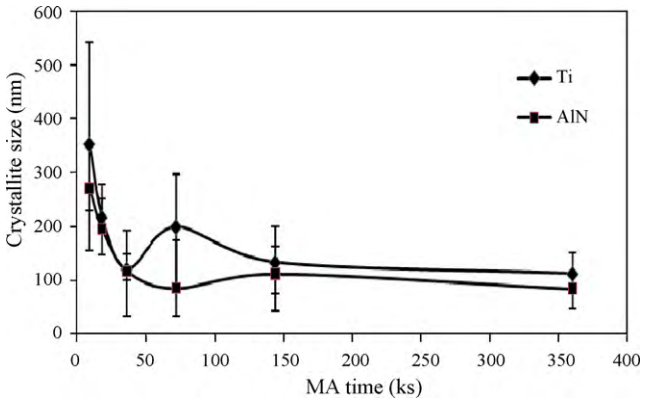

Fig. 7. Crystallite size of Ti and AlN particles at several MA times.

to smaller angles as stated by the Bragg equation. This explains the complicated behavior of the main peak position of titanium in XRD pattern.

As shown in Fig. 5 the nonlinear variation of interplanar distance of Ti(1 0 1) reveals the competition between two processes, i.e. dissolution of Al and N in Ti lattice. It can be seen that between 18 ks and 36 ks of milling, the increase in interplanar distance is a sign of the solution of N in Ti. This is consistent with Ti(1 0 1) shifting to lower angles (Fig. 4). However, with increased milling time, the dissolution of the aluminum dominates the dissolution of nitrogen in titanium lattice. In a good agreement with this claim, the (c/a) ratio also shows a considerable increase within this period of MA time (18–36 ks), which proves that nitrogen atoms dissolve in Ti lattice and dilate it (Fig. 6). The content of N dissolved in Ti lattice was estimated to be 1 at.% for 144 ks milling time according to the relation between lattice parameter and dissolved content of nitrogen[49]. It can be concluded that a minor part of the nitrogen atoms from decomposed AlN particles is dissolved into the Ti lattice to form Ti(Al,N) solid solution and leads to dilation of it, while the remaining N react with Ti to form TiN.

According to the above analysis, synthesis of nanocrystalline TiN by mechanical milling from Ti–AlN mixture included three stages. In the first stage, the ductile metal powder particles (Ti) got flattened, welded and formed lamellar structure by the ball-powder-ball collisions, while the brittle AlN particles got fragmented and dispersed into the ductile matrix. With prolonged milling time, the lamellae refined further and the brittle particles uniformly dispersed. The decreased particle size reduces the diffusion distance between particles and facilitates pipe diffusion. Diffusion is further aided by the increased defect density and a local rise in temperature. The combination of these effects would permit sufficient diffusion to occur in the interfacial regions between Ti and AlN particles of the nanocrystalline grains to form solid solutions and reduction of AlN under the effect of Ti. In other words, plastic deformation of Ti powder and refining by the ball-powder-ball collisions absorbed the nitrogen atoms from decomposed AlN particles on the newly created Ti surfaces. Nitrogen atoms are then incorporated in the interfaces formed by the pressure welding of the AlN–Ti powders on milling, followed by diffusing into powder matrices through grain boundaries and dislocations.

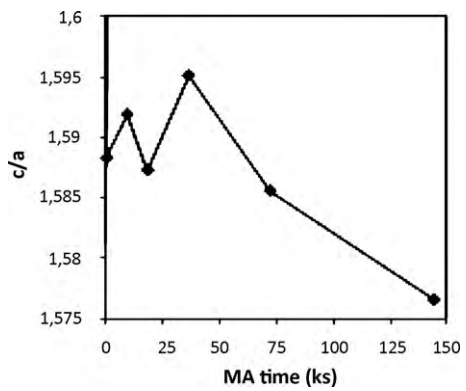

Fig. 6. The ratio of the Ti lattice parameters (c/a) vs. MA time.

By repeating the above process, a quasi-amorphous solid solution consisting of Ti,Al and N is formed in the powder matrix as the second stage of synthesis of TiN. Formation of nanocrystalline solid solutions can considerably broaden the X-ray diffraction peaks [7], as can be seen clearly in Fig. 1f and g.

The dissolved Al and N atoms diffuse into the Ti lattice, but they have opposite effects in Ti lattice; while dissolving the aluminum atoms decrease the lattice parameters of titanium, N cause it to increase. Meanwhile, almost all of the aluminum atoms dissolved in titanium in which a great number of cavities are produced, though only a minor amount of nitrogen dissolved in it.

In the last stage, the increase of energy stored in the composite powders induced by MA, caused N and titanium solid solution to interdiffuse and synthesize in situ TiN nanoparticles. It is worth to note that titanium atoms preferentially absorb nitrogen atoms as a result of the difference between diffusion coefficient of Al and N atoms. Therefore, the Ti-rich nitride would be formed. The radii of N, Ti and Al atoms are 0.07 nm, 0.1448 nm and 0.1431 nm [50], respectively, so nitrogen atoms diffuse mainly interstitially in the Ti lattice and should have a higher diffusion velocity than that of Al atoms which diffuse mainly by substitution. Because differences in diffusion velocities between Al and N atoms will result in a different gradient distribution in the diffusion direction, it can be assumed that titanium nitride was first formed in the nitrogen concentrated regions such as grain boundaries and then in the whole powder matrices.

The broadening of the titanium, AlN and also TiN peaks is considered to be due to the refinement effect of crystallite size and the increase in internal strain. The crystallite size of the Ti and AlN particles during MA calculated from the line width is shown in Fig. 7. It can be seen that there is a drastic decrease of particle size until 36 ks of milling time for both titanium and AlN particles, which is described on the basis of interaction of dislocation with hard and nondeformable aluminum nitride particles and generation of thermal dislocations caused by the mismatch between the coefficient of thermal expansion between the Ti and hard AlN particles [51]. Between 36 ks and 72 ks of MA time, cold welding is the prominent mechanism for titanium particles. Continued milling causes attainment of a steady state by 144 ks for both phases. This can be attributed to the cold welding of primary particles followed by

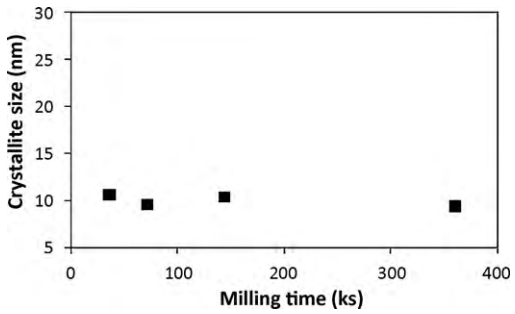

Fig. 8. Crystallite size of in situ formed TiN(2 0 0) phase at several MA times.

work hardening and thus activating the fracture mechanism. When welding and fracture mechanisms reach equilibrium, the steady state is achieved. Further milling up to 360 ks has no considerable effect on reducing the crystallite size. Nonetheless, it is important to note that after powder size stabilizer, microstructural refinement can still take place; this terminates at a later time, as can be seen in Fig. 7, within the 144–360 ks of milling time. A similar behavior was observed by Karagedov and Lyakhov, who reported the mechanochemical grinding of inorganic oxides [53]. Fig. 8 shows the crystallite size of TiN particles formed during milling which was calculated from the line width as a function of MA time. An average crystallite size of 10 nm was obtained for TiN particles, in accordance with the estimate of the Scherrer formula.

3.2. Effect of subsequent heat treatment on microstructure of powder mixture

In order to further study the structural evolution of the powder at elevated temperature, annealing experiments were performed. Fig. 9 shows XRD patterns of Ti–AlN powder mixture milled for 360 ks followed by annealing at different temperatures for 30 min under argon atmosphere. The XRD pattern of the powder after annealing at 650 °C (Fig. 9b) shows that the Ti peaks disappeared completely, suggesting that titanium solid solution was exhausted by reaction with AlN. However there is no evidence of the formation of more TiN at this temperature, perhaps due to the formation of very small content of TiN which cannot be detected by XRD. Increasing the annealing temperature up to the 850 °C leads to the in situ formation of TiN at $2\theta = 74.4^\circ$ and 78.16° during heat treatment. The presence of these two peaks of TiN can be interpreted as a phase transformation from supersaturated solid solution Ti(Al,N), which had been formed during MA. The vanishing of the AlN peak at

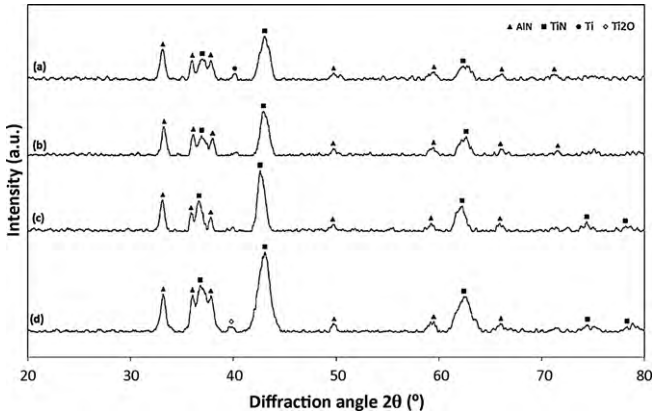

Fig. 9. XRD patterns of Ti + AlN mixture (a) milled for 100 h; (b) milled followed by annealing at 650 °C; (c) milled followed by annealing at 850 °C; (d) milled followed by annealing at 1050 °C.

Table 2
Calculated cell parameter of TiN(2 0 0) for 360 ks MA and annealing at different temperatures for 30 min together with literature standard.

Sample condition (360 ks of MA time)	Cell parameter of TiN, a (Å)
Annealed at 650 °C	4.1775
Annealed at 850 °C	4.1823
Annealed at 1050 °C	4.1858
Without annealing	4.1988
TiN[a]	4.2417
Al[a]	4.0494

[a] From JCPDS standard.

$2\theta = 71.75^\circ$ revealed more decomposition of AlN during annealing. It is believed that the following reaction occurs during annealing:

$$\mathrm{Ti(Al, N)} \rightarrow \mathrm{TiN(Al) or (Ti, Al)N} \quad (3)$$

That is, because of the low solubility of N in Ti lattice, the N released from Ti(Al,N) solid solution during the annealing, results in formation of in situ TiN particles. Table 2 shows the *fcc* lattice parameter of TiN(2 0 0) after milling and annealing for 30 min at different temperatures. The TiN phase is characterized by a lower (a) parameter when compared with the standard value (4.1988 Å for 360 ks of MA compare to the 4.241 Å from standard JCPDS); this indicates the solution of aluminum into the TiN lattice.

In addition, the increase in the lattice parameter of TiN with increased annealing temperatures confirms that TiN is closer to its stoichiometric characteristic (TiNx ($x = 0.42$–1)) [41] as expected. Further increase in temperature up to 1050 °C provides, no further detectable transformation; only a small amount of TiO_2 was detected due to the high temperature used for annealing, resulting in the possibility of oxidation. Moreover, with the increase in annealing temperature, the TiN and AlN peaks become sharper and of higher intensity because of stress release as well as grain growth. Fig. 10 illustrates the crystallite size of TiN particles after annealing at three different temperatures. Using the Scherrer equation, it can be deduced that the crystallite size of TiN is less than 14.62 nm with about 28% grain growth after annealing at 1050 °C compared to the case prior to annealing.

3.3. Morphological changes

The morphology of milled powders at different milling times is represented in Fig. 11. Photographs (a) and (b) are initial AlN and Ti powders, respectively. The as received AlN powder is polygonal, while Ti powder is spherical in shape. After 9 ks milling (Fig. 11c), particles with different shape and size were formed and hard AlN particles were seen to be pressed onto the Ti particles and cover the entire surface. After 18 ks milling, a few large particles of Ti consisting of smaller microwelded AlN particles with the presence of a lot of fine particles can be seen (Fig. 11d). After 36 ks milling, the

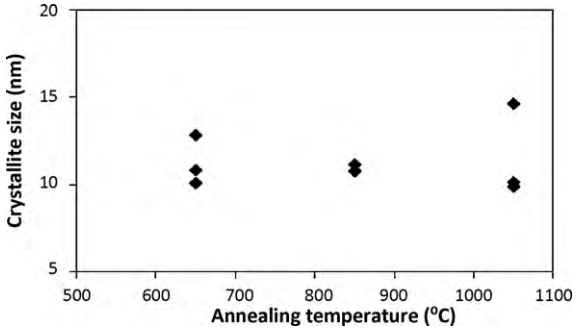

Fig. 10. Crystallite size of in situ formed TiN phase at different annealing temperatures.

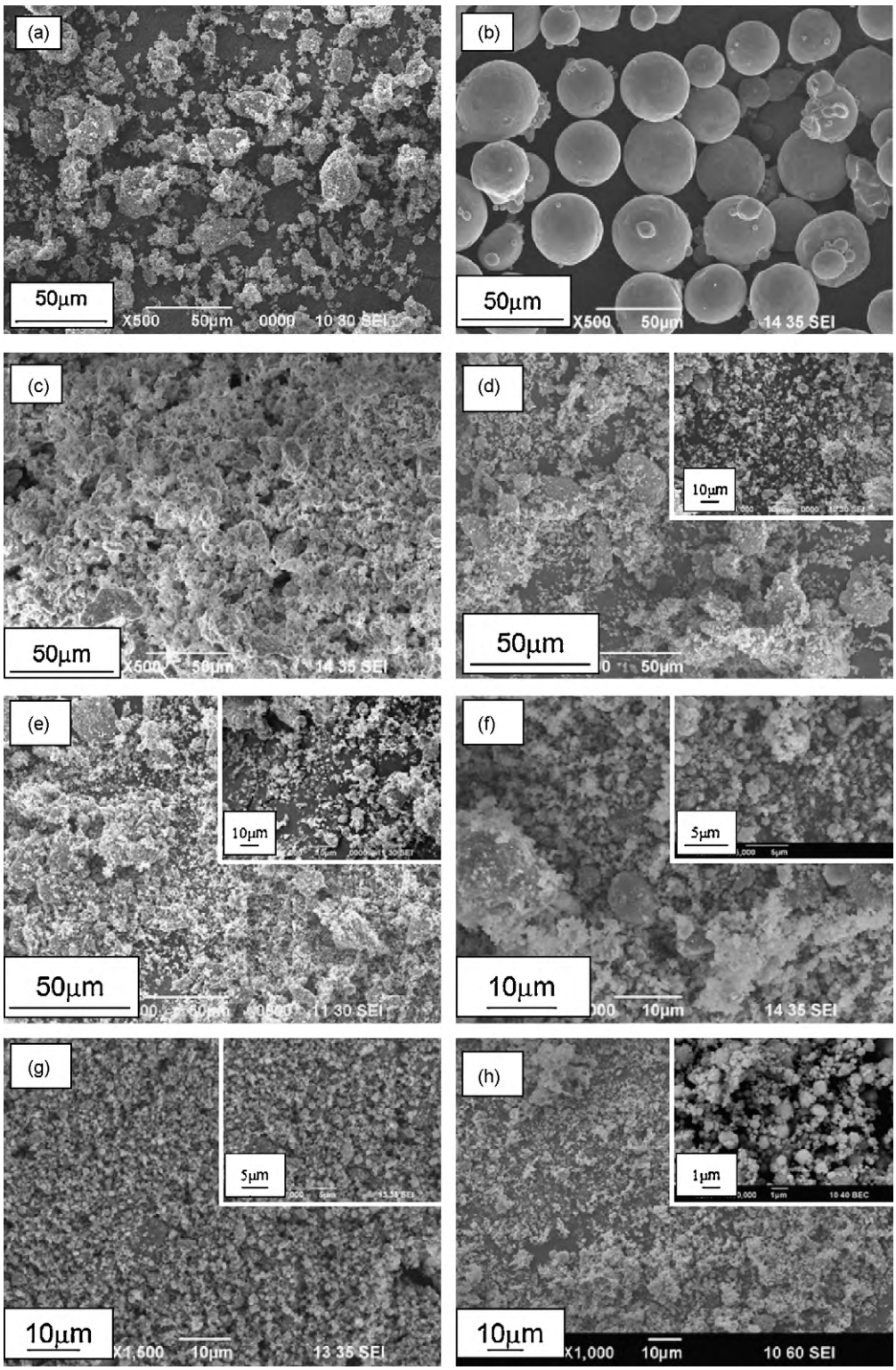

Fig. 11. SEM photographs of microstructures of as-milled powder with various milling times. (a) and (b) Initial powders of AlN and Ti, respectively; (c) after 9 ks milling; (d) after 18 ks milling; (e) after 36 ks milling; (f) after 72 ks milling; (g) after 144 ks milling; (h) after 360 ks milling.

powder has a broad distribution of irregular particles, and because of the fine sizes and quantities of fresh surfaces produced by MA process, the particles were likely to form agglomeration of granular and uniform particles as shown in Fig. 11e. The presence of TiN(2 0 0) peak at this milling time (Fig. 1) shows that Ti powders were deformed plastically and then fractured by the continuous ball to powder collisions and also by the presence of hard particles of AlN. This resulted in the extreme refinement of Ti and AlN powder particles, decrease in crystalline size of Ti and AlN, introduction of a large number of defects and fresh surface in both phases. This in turn accelerates the following absorption and diffusion process of nitrogen atoms from fine particles of AlN in titanium.

With increased milling time, AlN particles were trapped between the titanium particles, which can be attributed to the

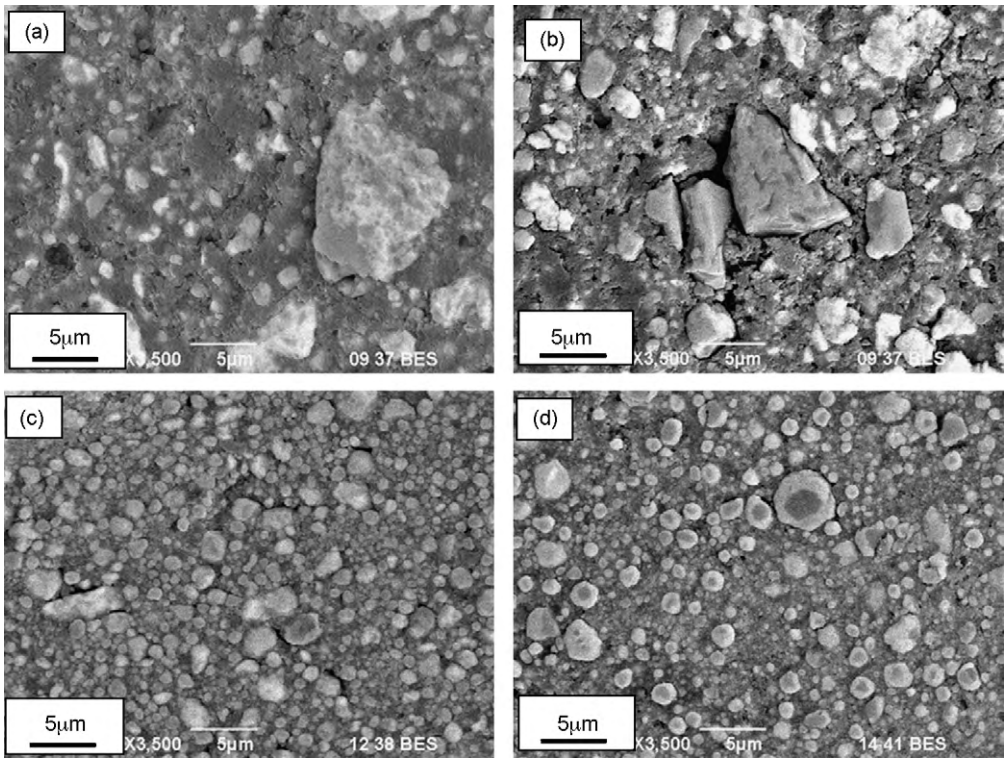

Fig. 12. The cross-sectional SEM micrographs the powders at different MA times: (a) 18 ks; (b) 36 ks; (c) 144 ks; (d) 360 ks.

repeated fracture and cold welding (Fig. 11f). This is in consistent with the results in Fig. 7. The presence of a few large particles of Ti would be fractured by the more intensive impacts due to the work hardening of the Ti. By continuing the milling, fracture governed welding, and the morphology transformed into completely equiaxed and very fine structure, a typical characteristic of particles at steady state (Fig. 7g). The reduction in crystalline size is induced by the formation of new defects particularly dislocations, resulting in formation of high dislocation density regions into the grains, piling up of grain boundaries or irregular clusters into the grains. Therefore, the subgrains are formed in the original grains, resulting in reduction of crystalline size [54]. Moreover, it has been reported that AlN particles can act as milling agent [55] and speed up the refining. The refinement of microstructure can be accelerated leading to a fast absorption rate of nitrogen atoms from AlN particles as can be seen in XRD patterns (Fig. 1f and g). Further milling, up to 360 ks has no considerable effect on the morphology (Fig. 11h); a similar phenomenon has been found that particle size maintains a steady level during MA [56–58].

Fig. 11h also shows a backscattered electron (BSE) image of 360 ks milled nanostructured composite powder. Fig. 12 illustrates the cross-sectional back scattered SEM micrographs of the powder particles after 18 ks, 36 ks, 144 ks and 360 ks of milling time. A layered composite structure of starting materials formed at early stage of MA can be seen in Fig. 11a and b. It is suggested that the formation of Ti(Al,N) solid solution begins to occur at these stages, consistent

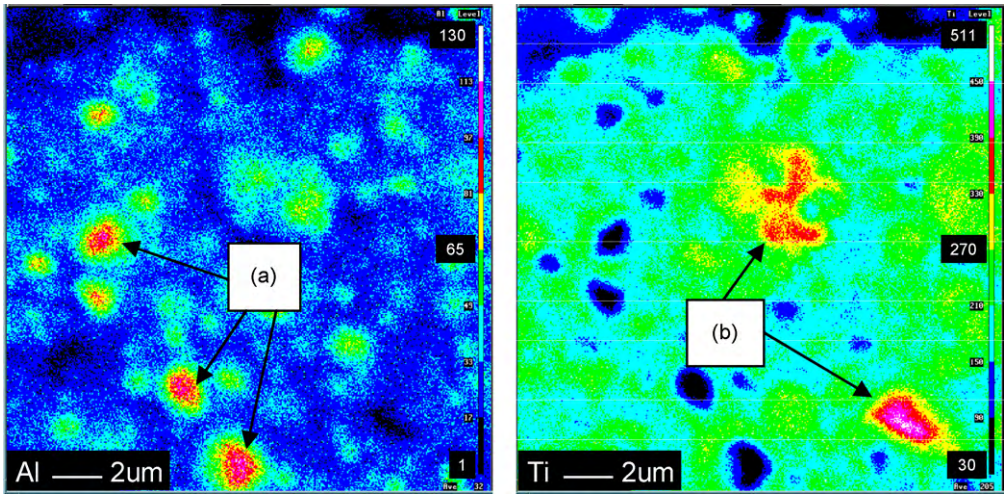

Fig. 13. Electron microprobe elemental maps for of Al and Ti for 360 ks MA sample. The colors correspond to count rates. The higher count rates indicate higher concentrations of the element(s) indicated. The spots marked as (a) and (b) indicate regions containing high concentration of Al and Ti, respectively. (For interpretation of the references to color in this figure legend, the reader is referred to the web version of the article.)

with the results in Fig. 4. As milling time increased, the layered structure is refined so that after 144 ks of milling, the layered structure disappeared due to increasing interdiffusion between the phases.

With increased milling time up to 360 ks, two phases are observed clearly. EPMA maps of the sample ball-milled for 360 ks distinguish the Ti- and Al-rich regions (Fig. 13). For instance, the region marked '(a)' indicates high concentrations of Al and N; the mark '(b)' indicates region enriched in Ti and N. Characterization of nitrogen was not possible due to the use of a 1 μm diameter beam for spot analyzing. The results of EDS and EPMA analysis confirm that this phase, AlN and TiN, is in agreement with XRD results.

It is interesting to note that no binary (with the exception of TiN) or ternary compounds like Ti_2AlN from Ti–Al–N system are being formed in the present study even after annealing (apart from a very small amount of Ti_3AlN and Ti_2N at the early stages of MA, detected in XRD analysis). The reason is presumed to the complete dissolving of aluminum in Ti lattice due to the selected equiatomic elemental powder mixture which is subjected to mechanical alloying and formation of solid solution.

4. Conclusions

AlN/TiN nanostructured composite was produced by high-energy ball mill and subsequent annealing of powder mixture containing Ti and AlN ingredients. The mechanochemical reaction between Ti and AlN took place in a gradual mode and led to the formation of nanostructured composite. The obtained results can be summarized as follows:

1. A part of AlN was found to be gradually reduced by Ti during MA and Ti(Al,N) solid solution formed after early stages of milling.
2. The particle size of supersaturated Ti(Al,N) solid solution and AlN reduced to submicron size and formed nanocrystalline structure as evident from XRD and SEM results.
3. The lattice parameter and interplanar distance of Ti shows that all of the decomposed Al dissolved in the Ti lattice by MA and causes its contraction, while only 1 at.% of N dissolves to form Ti(Al,N) solid solution and leads to its dilation and the remaining N reacts with Ti to form TiN.
4. Annealing of 360 ks MA powder leads to phase transformation as a result of increased thermal diffusivity, the formation of more TiN phase with more under-stoichiometric characteristic, as well as stress releasing and grain growth.

Acknowledgements

This work was supported by Global COE program, "Global Initiative Center for Pulsed Power Engineering", Kumamoto University. The authors also would like to thank L. Chen, G. Kennedy and W. Baerg for their kind cooperation and expert comments.

References

[1] J. Li, K. Hu, Y. Zhou, Mater. Sci. Eng. A 326 (2002) 270–275.
[2] R. Roj, J. Am. Ceram. Soc. 76 (1993) 2147–2174.
[3] N. Claussen, D.E. Garcia, R. Janssen, J. Mater. Res. 11 (1996) 2884–2888.
[4] K. Niihara, J. Ceram. Soc. Jpn. 99 (1991) 974–982.
[5] K.P. Rao, Y.J. Du, Mater. Sci. Eng. A 277 (2000) 46–56.
[6] D.L. Zhang, Prog. Mater. Sci. 49 (2004) 537–560.
[7] C. Suryanarayana, Prog. Mater. Sci. 46 (2001) 1–184.
[8] J.H. Shim, J.S. Byun, Y.W. Cho, Scripta Mater. 47 (2002) 493–497.
[9] R.N.P. Choudhary, K. Perez, P. Bhattacharya, R.S. Katiyar, Mater. Chem. Phys. 105 (2007) 286–292.
[10] C.C. Koch, Mater. Sci. Eng. A 244 (1998) 39–48.
[11] Z.H. Cai, D.H. Zhang, Mater. Sci. Eng. A 419 (2006) 310–317.
[12] A. Kobayashi, Surf. Coat. Technol. 132 (2000) 152–157.
[13] M. Zakeri, R. Yazdani-Rad, M.H. Enayati, M.R. Rahimipour, J. Alloys Compd. 403 (2005) 258–261.
[14] S.J. Hwang, J. Lee, Mater. Sci. Eng. A 405 (2005) 140–146.
[15] J. Li, F. Li, K. Hu, J. Mater. Process. Technol. 147 (2004) 236–240.
[16] F. Karimzadeh, M.H. Enayati, M. Tavoosi, Mater. Sci. Eng. A 486 (2008) 45–48.
[17] T. Mousavi, F. Karimzadeh, M.H. Abbasi, J. Alloys Compd. 467 (2009) 173–178.
[18] T. Bacci, L. Bertamini, F. Ferrari, F.P. Galliano, E. Galvanetto, Mater. Sci. Eng. A 283 (2000) 189–195.
[19] F.S. Shieu, L.H. Cheng, Y.C. Sung, J.H. Huang, G.P. Yu, Thin Solid Films 334 (1998) 125–132.
[20] J.P. Tu, L.P. Zhu, H.X. Zhao, Surf. Coat. Technol. 122 (1999) 176–182.
[21] S.J. Bull, Y.P. Sharkeev, S.V. Fortuna, L.A. Shulepov, A.J. Perry, J. Mater. Res. 16 (2001) 3293–3303.
[22] J.P. Tu, Corros. Sci. 42 (2000) 147–163.
[23] E. Salahi, J.G. Heinrich, Br. Ceram. Trans. 102 (4) (2003) 161–168.
[24] K.A. Khor, K.H. Cheng, L.G. Yu, F. Boey, Mater. Sci. Eng. A347 (2003) 300–305.
[25] K. Watari, H.J. Hwang, M. Toriyama, S. Kanzaki, J. Mater. Res. 14 (1999) 1409–1417.
[26] A.E. McHale, H.F. McMurdie, H.M. Ondik, Phase Equilibr. Diagrams Westerville (1994).
[27] R. Du, H. Okamura, R. Watanabe, J. Jpn. Soc. Powder Powder Metall. 50 (2003) 811–815.
[28] M. Tajika, H. Matsubara, W. Rafaniello, J. Mater. Sci. Lett. 20 (2001) 201–203.
[29] F. Cheng, Y. Sugahara, K. Kuroda, Appl. Organomet. Chem. 15 (2001) 710–716.
[30] T. Yasumoto, K. Yamakawa, N. Iwase, J. Ceram. Soc. Jpn. Int. Ed. 101 (1993) 944–948.
[31] W.B. Carter, M.V. Papageorge, J. Vaccine Sci. Technol. 10A (1992) 3460–3464.
[32] R.K. Brow, R.E. Loehman, A.P. Tomsia, Adv. Ceram. 26 (1989) 189–196.
[33] A.P. Tomsia, R.E. Loehman, Mater. Manuf. Process. 9 (1994) 547–561.
[34] M.G. Norton, J.M. Kajda, B.C.H. Steele, J. Mater. Res. 5 (1990) 2172–2176.
[35] A.H. Carim, R.E. Loehman, J. Mater. Res. 15 (1990) 1520–1529.
[36] C. Suryanarayana, M. Grant Norton, X-ray Diffraction: A Practical Approach, Plenum Press, NY, 1998.
[37] I. Barin, Thermochemical Data of Pure Substances, VCH Verlagsgellschaft, Weinheim, Germany, 1993.
[38] C. Suryanarayana, Intermetallics 3 (1995) 153–160.
[39] J.C. Oliveira, A. Manaia b, A. Cavalei, Thin Solid Films 516 (2008) 5032–5038.
[40] Z.A. Munir, Am. Ceram. Soc. Bull. 67 (1988) 342–349.
[41] ASM Handbook Alloy Phase Diagrams, vol. 3, 2nd ed., ASM International, 1990.
[42] O. Knacke, O. Kubaschewski, K. Hesselmann, Thermochemical Properties of Inorganic Substances II, 2nd ed., Springer-Verlag, Berlin, Heidelberg, 1991.
[43] B.L. Huang, R.J. Perez, E.J. Lavernia, M.J. Luton, Nanostruct. Mater. 7 (1996) 67–79.
[44] W.B. Pearson, G.V. Raynor (Eds.), A Handbook of Lattice Spacings and Structures of Metals and Alloys, vol. 4, Pergamon Press, Oxford, 1958.
[45] S. PalDey, S.C. Deevi, Mater. Sci. Eng. A 342 (2003) 58–79.
[46] T.D. Shen, C.C. Koch, Nanostruct. Mater. 5 (1995) 615–629.
[47] E. Galvanetto, F.P. Galliano, F. Borgioli, U. Bardi, A. Lavacchi, Thin Solid Films 384 (2001) 223–229.
[48] J.C. Oliveria, A. Manaia, A. Cavaleiro, Thin Solid Films 516 (2008) 5032–5038.
[49] H.A. Wriedt, J.L. Murray, Bull. Alloy Phase Diagrams 8 (1987) 378–388.
[50] R. Yue, Y. Wang, Y. Wang, C. Chen, Surf. Interface Anal. 27 (1999) 98–102.
[51] Z.H. Li, Handbook of Element Properties, Hebei People's Publishing House, China, 1995.
[53] G.R. Karagedov, N.Z. Lyakhov, KONA 21 (2003) 76–86.
[54] B. Gómez, E. Gordo, J.M. Torralba, Sci. Eng. A 430 (2006) 59–63.
[55] Z. Razavi Hesabi, A. Simchi, S.M. Seyed Reihani, Mater. Sci. Eng. A 428 (2006) 159–168.
[56] V. Shankar, L. Lu, M.O. Lai, JSME Int. J. A 3 (2003) 251–254.
[57] J. Li, K. Hu, Y. Zhou, 326, Mater. Sci. Eng. A (1992) 270–275.
[58] N.Q. Wu, Mater. Sci. Technol. 14 (1997) 287–292.